

# Supporting Information

## Giant enhancement of cathodoluminescence of monolayer transitional metal dichalcogenides in a van der Waals heterostructure

*Shoujun Zheng,<sup>†, #</sup> Jin-Kyu So,<sup>†, #</sup> Fucui Liu,<sup>‡</sup> Zheng Liu,<sup>‡</sup> Nikolay Zheludev,<sup>\*, †, §</sup> and  
Hong Jin Fan<sup>\*, †, ⊥</sup>*

<sup>†</sup>Centre for Disruptive Photonic Technologies, School of Physical and Mathematical Sciences & The Photonics Institute, Nanyang Technological University, Singapore 637371

<sup>‡</sup>School of Materials Science and Engineering, Nanyang Technological University, 639798, Singapore

<sup>§</sup>Optoelectronics Research Centre and Centre for Photonic Metamaterials, University of Southampton, Southampton SO17 1BJ, United Kingdom

<sup>⊥</sup>Division of Physics and Applied Physics, School of Physical and Mathematical Sciences,  
Nanyang Technological University, 637371, Singapore

<sup>#</sup>These authors contributed equally to this work.

\*Correspondence to: NZheludev@ntu.edu.sg, fanhj@ntu.edu.sg

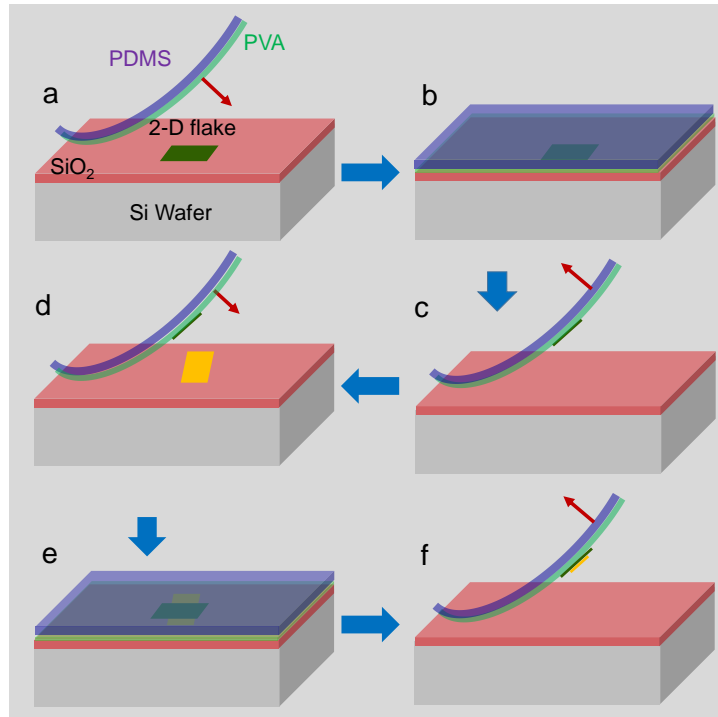


**Figure S1.** Schematics of the dry transfer process to fabricate the hBN/TMD/hBN vdW heterostructure.

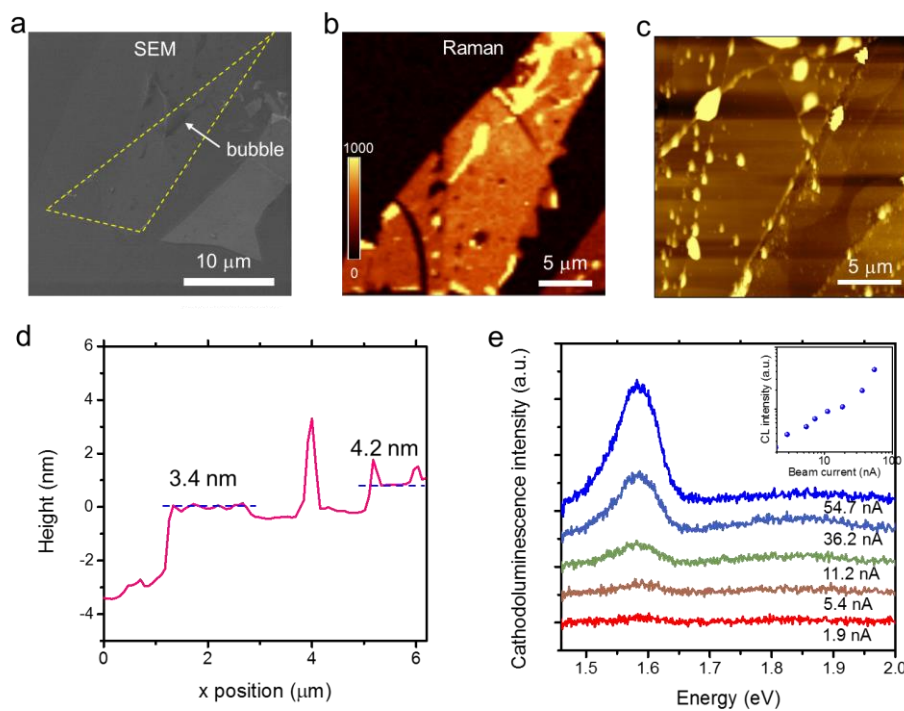
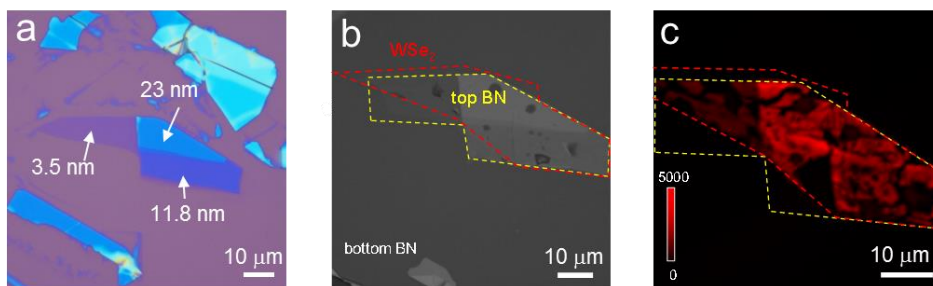


**Figure S2.** Characterization of the hBN/WSe<sub>2</sub>/hBN sample. (a) SEM image of the heterostructure. Yellow lines show the shape of the monolayer WSe<sub>2</sub>. Arrows indicate

the bubble generated during the transfer process and growing bigger after putting the sample into vacuum. (b) Raman mapping. (c) AFM topography and (d) profile of the sample in Fig. 2b. The thickness of the top hBN is around 4.2 nm. (e) Beam current dependent cathodoluminescence spectra. Inset is integrated intensity as a function of the beam current.

### Heterostructure with variable top hBN thickness



### Heterostructure with variable bottom hBN thickness

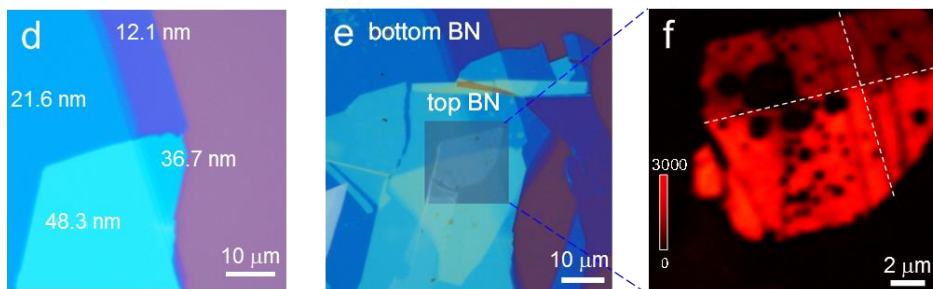


**Figure S3. Effect of the thickness of the top and bottom hBN layers.** (a) Optical image of the selected top hBN layer before transfer, which has three thickness regions as indicated, (b) The final sample of hBN/WSe<sub>2</sub>/hBN on Si/SiO<sub>2</sub> substrate and (c) the corresponding cathodoluminescence mapping. (d) Optical image of the selected bottom hBN layer before transfer, (e) the finished hBN/WSe<sub>2</sub>/hBN sample 3 on Si/SiO<sub>2</sub> substrate and (f) the corresponding cathodoluminescence mapping.

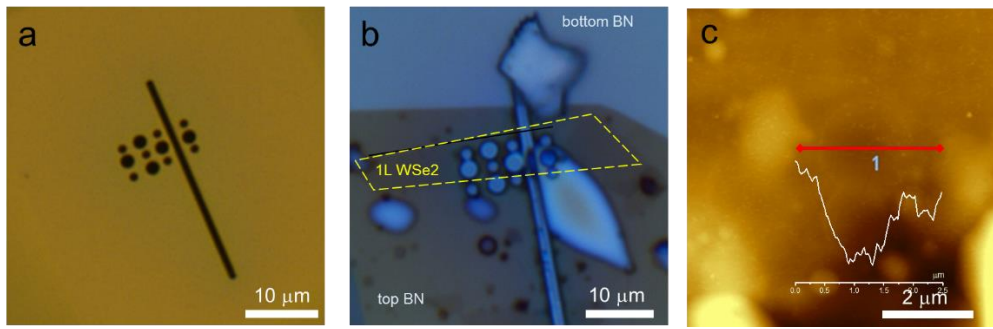


**Figure S4. hBN/WSe<sub>2</sub>/hBN sample on located on fabricated holes.** (a) Optical image of a Si substrate with holes fabricated by a focused ion beam. The holes have two diameters of 1 and 2  $\mu\text{m}$ . (b) Optical image of the hBN/WSe<sub>2</sub>/hBN sample transferred on top of the holes. (c) AFM topography mapping of the sample around holes. Inset: height profile along the line.

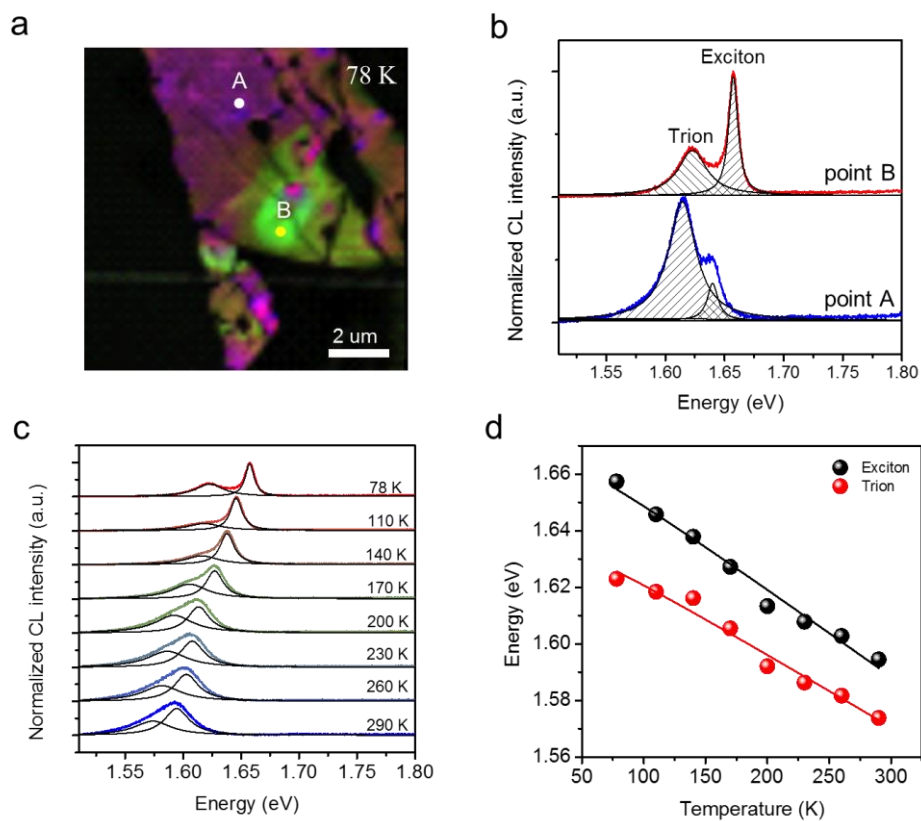


**Figure S5. Temperature dependent cathodoluminescence of hBN/WSe<sub>2</sub>/hBN vdW heterostructure.** (a) Cathodoluminescence wavelength mapping at 78 K. The green

and purple regions correspond to two frequency domains corresponding to the dominating exciton peak, respectively. (b) Cathodoluminescence spectra recorded from the two points in (a) showing both excitons and trions. (c) Temperature-dependent spectra and (d) plot of the peak positions of the excitons and trions as a function of temperature. Lines are the fittings according to a semiconductor band gap equation (see text).